

Article

Effect of Ultra-Fine Grinding on the Structure of Plant Raw Materials and the Kinetics of Melanin Extraction

Igor Lomovskiy , Ekaterina Podgorbunskikh *  and Oleg Lomovsky

Laboratory of Mechanochemistry, Institute of Solid State Chemistry and Mechanochemistry SB RAS, 630128 Novosibirsk, Russia; lomovsky@solid.nsc.ru (I.L.); lomov@solid.nsc.ru (O.L.)

* Correspondence: podgorbunskikh@solid.nsc.ru; Tel.: +7-913-712-7092

Abstract: Enhancing the extraction rate is one of the key objectives in optimization of extraction of substances from biogenic raw materials. Ultra-fine grinding of plant raw materials (to achieve particle size less than 300 μm) is a very appealing method for increasing the extraction rate using relatively simple equipment. However, this approach often fails to yield the desired result. This study focuses on the kinetics of melanin extraction from two types of raw materials: fungus *Ganoderma applanatum* and buckwheat husk. Particle size is shown to be just one of the key factors. The degree of order of plant-based feedstock strongly affects the intraparticle diffusion constants and can be a parameter controlling the diffusion rate. It has been shown that there exist optimal degrees of disorder of the crystal structure of plant raw materials, which have a dome-shaped dependence pattern and allow one to increase the diffusion coefficient by several dozen times. The kinetics of melanin extraction was described by some kinetic models that include the first order equation, the Baker and Lonsdale model, the Axelrud equation, and the Ritger–Peppas model.

Keywords: kinetic of extraction; kinetic models; diffusion constant; crystallinity index; melanin; *Ganoderma applanatum*; buckwheat husk; mechanical treatment



Citation: Lomovskiy, I.; Podgorbunskikh, E.; Lomovsky, O. Effect of Ultra-Fine Grinding on the Structure of Plant Raw Materials and the Kinetics of Melanin Extraction. *Processes* **2021**, *9*, 2236. <https://doi.org/10.3390/pr9122236>

Academic Editor: Pasquale Crupi

Received: 2 November 2021

Accepted: 9 December 2021

Published: 13 December 2021

Publisher's Note: MDPI stays neutral with regard to jurisdictional claims in published maps and institutional affiliations.



Copyright: © 2021 by the authors. Licensee MDPI, Basel, Switzerland. This article is an open access article distributed under the terms and conditions of the Creative Commons Attribution (CC BY) license (<https://creativecommons.org/licenses/by/4.0/>).

1. Introduction

Extraction of plant raw material is one of the basic processes used for obtaining organic matter. Manufacturing of more than 50% of active pharmaceutical ingredients, 70% of cosmetic ingredients, and 90% of dietary supplements starts with obtaining plant extracts [1].

Extraction is a heterogeneous process. The extraction yield can be increased by subjecting the liquid phase to treatment with temperature, ultrasound, microwave radiation, oscillating pressure, etc., during extraction [2]. Another approach to increasing extraction yield and rate that is equally important is to perform preliminary preparation of the solid phase, which often involves mechanical comminution. The general reasoning is as follows: particle size reduction is expected to raise the extraction rate due to increased surface area and fewer pathways of diffusion of the extractable matter inside raw material particles. However, numerous studies have shown that this dependence is displayed only for particles larger than 300–500 μm (e.g., [3–5]). When reducing the particle size, it should be taken into account that plant raw materials have a porous structure and intrapore diffusion makes a significant contribution (sometimes the key one) to the kinetics of the process [6,7].

Mechanical treatment is the main method for reducing particle size of plant raw materials. Not only does high-intensity mechanical treatment of the polymer composite matrix reduce particle size, but it also significantly alters the internal structure both at the macromolecular and macro levels [8]. Disordering of cell walls mainly facilitates diffusion; contrariwise, pore collapse makes extraction more complicated. These effects have almost the same magnitude; therefore, the dependence of the extraction kinetics on particle size can be nontrivial [9].

This study aimed to analyze the effect of the degree of disorder on the kinetics of polyphenol extraction for two types of raw material. The first type was fungus *Ganoderma applanatum*, a highly porous raw material. The second type was buckwheat husk, a raw material containing almost no conductive pores. Both types of raw material contain chemically related polyphenols (melanins having characteristic high-intensity absorption bands in the visible light spectrum).

2. Materials and Methods

2.1. Materials

The following plant raw materials and reagents were used in this study: *Ganoderma applanatum* and buckwheat husk, humic acid (CAS 1415-93-6, technical, Sigma Aldrich, Moscow, Russia), hydrochloric acid (Sigma Aldrich, Moscow, Russia), and tris(hydroxymethyl)aminomethane (ACS reagent, $\geq 99.8\%$, MERCK KGaA, Darmstadt, Germany).

Fruiting bodies of *Ganoderma applanatum* and buckwheat husk were collected in September 2021 in the Gorno-Altai botanical garden, an Altai Branch of the Central Siberian botanical garden (SB RAS) ($51^{\circ}37'21.0''$ N $85^{\circ}42'16.0''$ E, Altai, Russia).

2.2. Mechanical Treatment

Mechanical treatment of model raw materials was used to obtain samples of practically the entire range of particle sizes and degrees of disordering. Various degrees of disordering and particle sizes reduction of the material can be achieved by using equipment with different types of mechanical action on the structure.

Mechanical pretreatment of raw materials was conducted in a laboratory-scale attritor (manufactured at the Institute of Solid State Chemistry and Mechanochemistry, SB RAS, Novosibirsk, Russia) filled with steel grinding bodies (9 mm in diameter) and equipped with a thermostat system. The temperatures of the thermostat circuit were room temperature and 95°C . The treatment duration was 10 and 20 min; the rotor speed was 600 rpm.

Mechanical treatment was conducted on an AGO-2 laboratory-scale water-cooled planetary ball mill (grinding body acceleration was 200 m/s^2 ; the rotational speed of the reactors was 630 rpm). The steel grinding bodies used were 5 mm in diameter and weighed 200 g. Weight of the treated material was 10 g; the pretreatment duration was 2, 4, 8, 12, and 18 min.

Mechanical treatment was carried out on an RM-20 flow-through centrifugal roller mill (shear mode) (manufactured at the Institute of Solid State Chemistry and Mechanochemistry, SB RAS, Novosibirsk, Russia). Steel rollers with zero eccentricity fixed on driving shafts and mechanically affecting the treated material with a fixed intensity were used as grinding bodies. The operating conditions were as follows: the raw material feed rate was 1.0 kg/h and the rotor speed was 900 rpm. The temperature in the cooling system was 50°C .

Mechanical treatment was conducted on an Desintegraator Tootmise OU Dezi-11 Mill (Estonia) equipped with a setup ensuring liquid nitrogen pre-cooling of the material. The rotor speed was 6000 rpm.

2.3. Structure and Morphology Analysis

The crystallinity degrees of *Ganoderma applanatum* and buckwheat husks were determined by X-ray diffraction (XRD) analysis. X-ray studies were performed on a D8 Advance powder diffractometer (Bruker, Karlsruhe, Germany) with monochromatic $\text{CuK}\alpha$ radiation (wavelength, 1.5406 \AA) in the Bragg–Brentano geometry. The analysis was conducted in a range of 2θ angles ($5\text{--}60^{\circ}$) at a voltage of 40 kV and current of 40 mA.

The crystallinity index was calculated in accordance with the Segal's method using the following formula [10]:

$$CI = \frac{I_{200} - I_{min}}{I_{200}} * 100\% \quad (1)$$

where CI is the crystallinity index; I_{200} is the intensity of (200) reflection; and I_{min} is the minimum between the (110) and (200) reflections.

The particle sizes of *Ganoderma applanatum* and buckwheat husks after grinding were measured on a CAMSIZER X2 optical analyzer (Retsch GmbH, Haan, Germany) with a detection threshold of 0.8–8000 μm and compressed air dispersion module (pressure 50 kPa). The average particle size was calculated using the image analysis method in compliance with ISO standard 13322-2:2006. The spherical shape factor b/l is the ratio of the minimum to maximum inscribed chords [11].

2.4. Studying the Extraction Kinetics

The extraction kinetics were studied spectrophotometrically. An aqueous solution of tris(hydroxymethyl)aminomethane (pH = 9.0) was added to the accurately weighed sample (1 g) of plant raw material. Mixing on a magnetic stirrer was performed in glass thermostats at 50.0 ± 0.2 °C for 5 h. A 1 mL sample was collected after 30 min, 60 min, and then every hour of extraction (until extraction was completed for a total of 6 h). The sample was filtered through a filter paper, and fine particles were precipitated via centrifugation (5500 rpm, 10 min). Each measurement was performed in five replicates.

Spectrophotometric analysis was conducted on a LOMO SF-2000 spectrophotometer (LOMO Ltd., St. Petersburg, Russia) at a wavelength of 465 nm. Humic acid at a concentration of 30–150 mg/L ($R^2 = 0.9888$ at 30–300 mg/L) was used as a reference. The calibration curve was fitted by a curve with $R^2 = 0.9996$.

2.5. Mathematical Models

If an extraction process is viewed as isolating substances from the matrix, several dissolution theories have been elaborated for such processes. We have chosen some of them.

Standard First Order Equation, based on the Second Fiks's Law:

$$C = C_0 * \left(1 - e^{-\frac{Dt}{r}}\right), \quad (2)$$

where

C is the concentration in the solution at the instant t (mg/mL);

C_0 is the equilibrium concentration at $t \rightarrow \infty$ (mg/mL);

D is the diffusion constant ($\mu\text{m}^2/\text{min}$);

r is the characteristic diffusion distance (equal to the particle radius (μm) in our case); and t is time (min) [12,13].

The first order equation was also used for running calculations for the total extraction kinetics after the steady-state mode had been attained (1–4 h).

Modification of the First Order Equation: The Baker and Lonsdale Model Taking into Account the Particles' Spherical Shape:

$$\frac{3}{2} \left[1 - \left(1 - \frac{M_t}{M_\infty} \right)^{2/3} \right] - \frac{M_t}{M_\infty} = \frac{3D_m C_{ms}}{r_0^2 C_{Init}} t, \quad (3)$$

where

M_t is the amount of the drug released at the time t (mg);

M_∞ is the amount released at an infinite time (mg);

D_m is the diffusion coefficient ($\mu\text{m}^2/\text{min}$);

C_{ms} is the solubility of the drug in the matrix (mg/mL);

r_0 is the radius of the spherical matrix (μm);

C_{Init} is the initial concentration of the drug in the matrix (mg/mL); and t is time (min) [14].

Modification of the First Order Equation: The Axelrud Equation Taking into Account Particles' Non-Sphericity:

$$\lg(C - C_1)/(C_{init} - C_1) = \lg B_i - 0.434\mu_i^2 Dt/R^2, \quad (4)$$

where

C_{init} is the initial concentration in the solid phase (mg/mL);

C is the concentration in a solid state (body) at the instant t (mg/mL);

C_1 is the concentration in the solution at the instant t (mg/mL);

B_i is the constant shape factor of a particle (a dimensionless quantity);

D is the effective diffusion coefficient in the pores of the solid phase ($\mu\text{m}^2/\text{min}$);

R is the size of solid particles (μm);

μ_i are the roots of the characteristic equation (a dimensionless quantity); and

t is the time (min) [15].

Solid-state diffusion and non-steady state diffusion may fail to follow the Fick law; therefore, we additionally used an empirical equation based on the power law (namely, the Ritger–Peppas model).

The Ritger–Peppas Model:

$$f_i = \frac{M_i}{M_\infty} = Kt^n, \quad (5)$$

where

f_i is the amount of drug released (mg);

M_∞ is the amount of drug in the equilibrium state (mg);

M_i is the amount of drug released over time t (mg);

K is the constant of incorporation of structural modifications and geometrical characteristics of the system n as a function of time t (min^{-1}); and

t is time (min) [16].

The reliability of the model was controlled using the simplest assessment method, the least-squares correlation coefficient (R^2).

3. Results and Discussion

3.1. Structure and Morphology Analysis

Characteristics of the initial raw material pre-ground on a cutting mill were as follows: crystallinity of the untreated *Ganoderma applanatum* was $80 \pm 1\%$, $b/l = 0.54$, average particle size was $250 \mu\text{m}$; crystallinity of untreated buckwheat husk was $65 \pm 2\%$, $b/l = 0.50$, average particle size was $1358 \mu\text{m}$.

Different depths of disorder of the structure of plant raw material were attained by mechanical treatment in activator mills where different types of mechanical action were employed (different variations of free and constrained impact or abrasion-shear type of mechanical impact). Table 1 lists the size and shape characteristics after mechanical pretreatment.

The data listed in Table 1 show that mechanical treatment gives rise to particles characterized by a sufficiently broad range of size and shape, which will allow one to study the kinetics in almost the entire range of generally applied degrees of raw material pretreatment. The resulting range almost completely covers the size of particles produced by ultra-fine grinding of this type of materials. A common trend is observed for both groups of study objects: reduction of particle size is also accompanied by a decrease in crystallinity index.

Table 1. Size and shape characteristics of particles of the analyzed raw materials.

No.	Method of Mechanical Treatment	Average Particle Size, μm	Spherical Shape Factor b/l (Krumbein and Sloss)	Crystallinity Index, %
<i>Ganoderma applanatum</i>				
1	Attritor, 10 min	114	0.65	75 ± 1
2	Attritor, 20 min	85	0.64	73 ± 2
3	AGO-2, 2 min	130	0.61	74 ± 1
4	AGO-2, 4 min	84	0.66	66 ± 2
5	AGO-2, 8 min	25	0.71	62 ± 2
6	AGO-2, 12 min	21	0.74	57 ± 3
7	AGO-2, 18 min	20	0.74	53 ± 3
8	Desi-11, 2 times	133	0.63	77 ± 1
9	Desi-11, 3 times	133	0.63	71 ± 2
Buckwheat husk				
1	Attritor, 20 min, 95 °C	529	0.55	51 ± 4
2	Desi-11, liquid nitrogen, 2 times	300	0.65	56 ± 3
3	Desi-11, liquid nitrogen	262	0.57	64 ± 2
4	AGO-2, 12 min	35	0.74	27 ± 4
5	Attritor, 20 min	398	0.50	45 ± 3
6	PM-20	93	0.63	52 ± 3

By using mechanical treatment of *Ganoderma applanatum*, the average particle size can be significantly changed due to disruption of conducting channels.

After primary preparation, buckwheat husk particles have a rectangular shape ($b/l = 0.5$). Mechanical treatment in the attritor and free-impact deactivator does not ensure any significant comminution compared to treatment in the PM-20 ensuring an abrasion-shear mechanical action and impact-shear mechanical action on an AGO-2 planetary activator where the particles after activation acquire a more spherical shape ($b/l > 0.6$) and become disordered.

3.2. The First Order Equation

The standard first order equation (Equation (2)) is the most common method for describing the extraction kinetics. Table 2 summarizes the results of fitting using this equation. Here and below, the samples are listed in order of descending crystallinity index of cellulose.

The reported data show that the first order equation describes the extraction kinetics with low correlation coefficients. The R^2 value is 0.964 in only one case, whereas in most cases R^2 is <0.9 , thus suggesting that the first order equation is hardly applicable under these extraction conditions.

We have put forward a hypothesis that the non-steady state of the process is the reason behind the low correlation coefficients. For this purpose, the data were processed only until the midpoint of the process (within 1–4 h). One can notice that this approach generally increases the correlation coefficients but fails to provide substantial improvement and does not allow one to use this model to properly analyze the kinetic curves. The result is sufficiently evident, as it was inadequate description of the kinetic extraction curves using the first order equation that had spurred the researchers towards elaborating a number of other models.

Table 2. The diffusion constant according to the first order equation as a function of particle size and crystallinity index.

No.	Crystallinity Index, %	Average Particle Size, μm	D Fick $\times 10^6$, $\mu\text{m}^2/\text{min}$	R ²	D Fick 4 Point $\times 10^6$, $\mu\text{m}^2/\text{min}$	R ²
<i>Ganoderma applanatum</i>						
1	75 \pm 1	114	2.07	0.914	1.56	0.891
3	74 \pm 1	130	1.27	0.895	1.40	0.847
2	73 \pm 2	85	2.10	0.736	1.98	0.860
8	77 \pm 1	133	1.59	0.917	2.17	0.964
9	71 \pm 2	133	1.45	0.918	1.21	0.848
4	66 \pm 2	84	1.62	0.875	1.88	0.829
5	62 \pm 2	25	8.57	0.880	7.09	0.898
6	57 \pm 3	21	9.07	0.823	8.86	0.749
7	53 \pm 3	20	4.53	0.858	5.07	0.738
Buckwheat husk						
3	64 \pm 2	262	0.65	0.858	0.82	0.807
2	56 \pm 3	300	0.83	0.844	0.95	0.815
6	52 \pm 3	93	3.97	0.924	4.29	0.874
1	51 \pm 4	529	0.50	0.815	0.59	0.711
5	45 \pm 3	398	0.65	0.729	0.63	0.875
4	27 \pm 4	34	19.73	0.818	22.32	0.789

3.3. The Baker and Lonsdale Model and the Axelrud Model

We have attempted to fit the extraction kinetics using the models that view particles as being completely spherical and take into account their non-sphericity; the data are listed in Table 3.

Table 3. The diffusion constants according to the Baker and Lonsdale model as well as the Axelrud model as a function of particle size and crystallinity index.

No.	Crystallinity Index, %	Average Particle Size, μm	D Baker Lonsdale $\times 10^3$, $\mu\text{m}^2/\text{min}$	R ²	D Axelrud $\times 10^3$, $\mu\text{m}^2/\text{min}$	R ²
<i>Ganoderma applanatum</i>						
1	75 \pm 1	114	36.9	0.955	90.7	0.946
3	74 \pm 1	130	33.7	0.920	87.1	0.918
2	73 \pm 2	85	23.8	0.923	41.3	0.962
8	77 \pm 1	133	47.0	0.932	134.7	0.953
9	71 \pm 2	133	57.2	0.950	93.5	0.956
4	66 \pm 2	84	14.7	0.945	34.4	0.936
5	62 \pm 2	25	1.7	0.968	4.0	0.930
6	57 \pm 3	21	1.3	0.964	2.6	0.963
7	53 \pm 3	20	0.9	0.883	1.3	0.923
Buckwheat husk						
3	64 \pm 2	262	98.2	0.907	367.8	0.936
2	56 \pm 3	300	328.0	0.964	777.6	0.925
6	52 \pm 3	93	56.6	0.964	122.9	0.960
1	51 \pm 4	529	1113.0	0.910	1277.1	0.941
5	45 \pm 3	398	352.4	0.912	1079.6	0.931
4	27 \pm 4	34	19.1	0.814	34.6	0.920

The data listed in Table 3 demonstrate that correlation coefficients for fitting the extraction kinetics using the Baker equation and the Lonsdale model (Equation (3)) are generally higher than those obtained using the first order equation; the Axelrud model (Equation (4)) provides a slightly better description of the extraction process. For both models, the correlation coefficients are higher than 0.91, being 0.943 on average. Therefore,

it can be considered that both models used for process description are characterized by identical reliability.

Analyzing the dependence between the diffusion coefficient and crystallinity index will further provide identical qualitative results; therefore, in the text below we will discuss only the Baker and Lonsdale model.

Figure 1 shows a graphical image of the diffusion coefficient as a function of the crystallinity index.

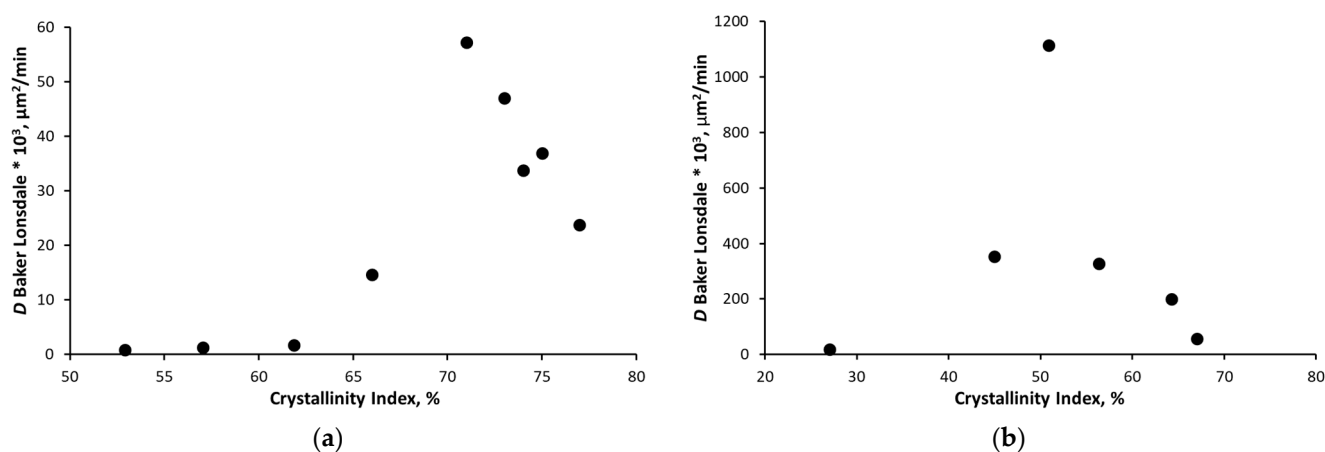


Figure 1. The diffusion coefficient according to the Baker Lonsdale model as a function of the crystallinity index of (a) *Ganoderma applanatum* and (b) buckwheat husk.

In both cases, the dependence pattern of the diffusion coefficient is dome-shaped. Previously (Table 1), we showed that there is a common dependence trend: the crystallinity index of raw material declines with decreasing particle size. If we view the overall process instead of taking into account that these data were obtained using different methods, the following trend can be seen:

1. Fine grinding reduces the degree of order of the samples.
2. As the crystallinity index decreases, the diffusion coefficient first significantly grows and then decreases down to the values even lower than those observed for the almost untreated raw material.
3. In any of the diffusion models under consideration, the flux of matter $j \approx \text{const} \cdot D/R^2$. Therefore, at deep degrees of disorder, the effects of size reduction and drop in the diffusion coefficient are oppositely directed and eventually lead to the following phenomenon: the flux of matter consisting of disordered fine particles is comparable to the flux of matter consisting of significantly larger particles characterized by larger crystallinity index.

The dome-shaped dependence of the diffusion constant on crystallinity index per se is not evident but can be explained. We have earlier shown [9] using the model system that high-intensity mechanical treatment first causes only cell wall disordering accompanied by a rise in the diffusion constant; then such processes as disruption of the porous structure of plant raw material, destruction of diffusion channels, and collapse of cavities (in which diffusion proceeds much easier than in the cell wall) start.

From the perspective of extractive processes, the raw material containing a large number of conducting channels (*Ganoderma applanatum*) is more sensitive to mechanical treatment, and destruction of conducting channels starts at an appreciably early stage (when the crystallinity index decreases by 10% of the initial value). Buckwheat husk is a raw material containing an insignificant number of conducting channels; therefore, the drop in diffusion rate starts only once the cavities (voids that were formed when the cellular contents were dried) had already collapsed. Therefore, the drop in diffusion rate starts after the crystallinity index is changed by 20%.

3.4. The Ritger–Peppas Model

An analysis of the kinetic curves using the Ritger–Peppas model yields interesting data (Table 4).

Table 4. The kinetic constant and diffusion exponent according to the Ritger–Peppas model as functions of particle size and crystallinity index.

No.	Crystallinity Index, %	Average Particle Size, μm	K Ritger–Peppas, $1/\text{min}$	n Ritger–Peppas, $\mu\text{m}^2/\text{min}$	R^2
<i>Ganoderma applanatum</i>					
1	75 ± 1	114	2.61	0.161	0.902
3	74 ± 1	130	2.51	0.125	0.925
2	73 ± 2	85	2.10	0.114	0.960
8	77 ± 1	133	2.72	0.177	0.956
9	71 ± 2	133	2.65	0.161	0.936
4	66 ± 2	84	2.37	0.113	0.938
5	62 ± 2	25	2.32	0.128	0.953
6	57 ± 3	21	2.03	0.100	0.947
7	53 ± 3	20	1.49	0.040	0.933
Buckwheat husk					
3	64 ± 2	262	3.62	0.256	0.925
2	56 ± 3	300	3.42	0.292	0.959
6	52 ± 3	93	2.83	0.241	0.962
1	51 ± 4	529	2.90	0.215	0.911
5	45 ± 3	398	3.44	0.259	0.958
4	27 ± 4	34	1.80	0.171	0.977

The reported correlation coefficients demonstrate that this model can also be formally used to analyze the kinetic data. However, it has significant limitations. The benefit of using the Ritger–Peppas model is that it yields not only the extraction rate constant K , but also the power coefficient n . The following boundary conditions are typically used when interpreting the data: $n = 0.43$ – 0.5 —Fickian diffusion; when $0.5 < n < 1$, the model is non-Fickian or there is anomalous transport, and the mechanism of drug release is governed by diffusion and swelling. The diffusion and swelling rates are comparable when $n > 1$, constituting an extreme form of transport. During the sorption process, tension and breaking of the polymer occurs.

In our case, the power coefficient n is 0.04 – 0.3 . A certain deviation of the power coefficient below 0.43 can be attributed to particle non-sphericity; however, one can see from Table 1 that the b/l ratio = 0.5 – 0.75 , whereas the model is supposed to provide adequate results up to $b/l = 0.1$ [17].

Unfortunately, no good interpretation of the processes for $n < 0.43$ (like in our case) has been provided yet. Therefore, it is impossible to adequately analyze the constants. However, it is fair to assume that such a significant decrease in power coefficients n (i.e., deceleration of the process compared to the standard Fickian diffusion) occurs due to the fact that the target substance (melanin) interacts with insoluble matrix components during its diffusion through the matrix. For example, it is reversibly sorbed onto lignin. A similar process has earlier been demonstrated for other systems (e.g., [18]).

It has previously been shown for model systems that high-intensity mechanical treatment can alter the chemical composition of the surface towards higher lignin concentration [19]. The functional groups in melanin, such as $-\text{OH}$, $-\text{NH}$, and $-\text{COOH}$, allow the formation of strong hydrogen bonding with polymer chains containing polar groups of lignin [20]. Melanin can form appreciably strong bonding with lignin. In our case, the power coefficient n drops with decreasing crystallinity index, being indirect evidence of the fact that melanin extraction is a process complicated by sorption of the target substance on lignin matrix.

4. Conclusions

1. The kinetics of melanin extraction from *Ganoderma applanatum* and buckwheat husk is adequately fitted by the extraction equations based on Fickian diffusion with allowance for the particle shape-factor (the Baker and Lonsdale model, the Axelrud model).
2. An analysis of the kinetic curves using the aforementioned models demonstrates that mechanical treatment can significantly alter the diffusion constants of melanin in the environment. As crystallinity index of cellulose contained in the raw material drops, diffusion is initially facilitated due to cell wall disordering. Further drop in the diffusion coefficient can be explained by destruction of the porous structure.
3. A significant decline in the diffusion coefficient upon substantial disordering explains why ultra-fine grinding does not necessarily causes a significant increase in the rate of extraction of the components of plant raw material.
4. There are optimal degrees of disorder that allow one to increase the diffusion coefficient several dozen times compared to the diffusion coefficients of the untreated raw material and highly disordered raw material. For *Ganoderma applanatum* and buckwheat husk, the optimum values correspond to Segal crystallinity index of cellulose being 71% and 51%, respectively.
5. An analysis using the Ritger–Peppas power-law model demonstrates that along with diffusion, there occur processes significantly decelerating it, including interaction between melanin and insoluble lignin contained in cell walls.

Author Contributions: Conceptualization, I.L. and O.L.; methodology, I.L.; validation, I.L. and O.L.; formal analysis, I.L. and E.P.; investigation, I.L. and E.P.; resources, I.L. and O.L.; data curation, I.L.; writing—original draft preparation, E.P.; writing—review and editing, E.P.; visualization, E.P.; supervision, O.L.; project administration, I.L. and O.L.; funding acquisition, O.L. All authors have read and agreed to the published version of the manuscript.

Funding: This research was supported by the Russian Science Foundation (project no. 21-13-00046).

Institutional Review Board Statement: Not applicable.

Informed Consent Statement: Not applicable.

Conflicts of Interest: The authors declare no conflict of interest.

References

1. Both, S.; Strube, J.; Cravatto, G. Mass transfer enhancement for solid-liquid extractions. In *Green Extraction of Natural Products: Theory and Practice*; Chemat, F., Strube, J., Eds.; Wiley-VCH Verlag GmbH & Co. KGaA: Weinheim, Germany, 2015; Volume 4, pp. 101–144. [[CrossRef](#)]
2. Vorobiev, E.; Chemat, F.; Lebovka, N. *Enhancing Extraction Processes in the Food Industry*, 1st ed.; CRC Press: Boca Raton, FL, USA, 2012. [[CrossRef](#)]
3. Babenko, Y.I.; Ivanov, E.V. Optimizing the intensification of extraction. *Theor. Found. Chem. Eng.* **2012**, *46*, 149–152. [[CrossRef](#)]
4. Yeop, A.; Sandanasamy, J.; Pang, S.F.; Abdullah, S.; Yusoff, M.M.; Gimbin, J. The effect of particle size and solvent type on the gallic acid yield obtained from *Labisia pumila* by ultrasonic extraction. *MATEC Web Conf.* **2017**, *111*, 02008. [[CrossRef](#)]
5. Patrautănu, O.A.; Lazar, L.; Popa, L.I.; Volf, I. Influence of particle size and size distribution on kinetic mechanism of spruce bark polyphenols extraction. *Cellul. Chem. Technol.* **2019**, *53*, 71–78. [[CrossRef](#)]
6. Delgado, J.M.P.Q. *Heat and Mass Transfer in Porous Materials—Diffusion Foundations*; Trans Tech Publications Ltd.: Zurich, Switzerland, 2016.
7. Luikov, A.V. *Heat and Mass Transfer in Capillary-Porous Bodies*; Pergamon Press: Oxford, UK, 1966.
8. Lomovskiy, I.; Bychkov, A.; Lomovsky, O.; Skripkina, T. Mechanochemical and size reduction machines for biorefining. *Molecules* **2020**, *25*, 5345. [[CrossRef](#)] [[PubMed](#)]
9. Lomovskiy, I.; Makeeva, L.; Podgorbunskikh, E.; Lomovsky, O. The Influence of Particle Size and Crystallinity of Plant Materials on the Diffusion Constant for Model Extraction. *Processes* **2020**, *8*, 1348. [[CrossRef](#)]
10. Segal, L.; Creely, J.J.; Martin, A.E.; Conrad, C.M. An empirical method for estimating the degree of crystallinity of native cellulose using the X-ray diffractometer. *Text. Res. J.* **1959**, *29*, 786–794. [[CrossRef](#)]
11. Krumbein, W.C.; Sloss, L.L. *Stratigraphy and Sedimentation*, 2nd ed.; W.H. Freeman and Company: San Francisco, CA, USA, 1963.

12. Bruschi, M.L. 5—Mathematical models of drug release. In *Strategies to Modify the Drug Release from Pharmaceutical Systems*; Bruschi, M.L., Ed.; Woodhead Publishing: Sawston, Cambridge, UK, 2015; Volume 5, pp. 63–86. [[CrossRef](#)]
13. Nedich, R.L.; Kildsig, D.O. Mechanism of dissolution I: Mathematical interpretation of concentration gradients developed during dissolution of a solid. *J. Pharm. Sci.* **1972**, *61*, 214–218. [[CrossRef](#)] [[PubMed](#)]
14. Baker, R.W.; Lonsdale, H.S. Controlled release: Mechanisms and rates. In *Controlled Release of Biologically Active Agents*; Taquary, A.C., Lacey, R.E., Eds.; Plenum: New York, NY, USA, 1974; pp. 15–71.
15. Axelrud, G.A.; Lysyansky, V.M. *Ekstragirovaniye (Sistema Toordoye Telo—Zhidkost') [Extraction, a Solid-Liquid System]*; Leningrad Press: Leningrad, Russia, 1974. (In Russian)
16. Ritger, P.L.; Peppas, N.A. A simple equation for describing of solute release. I. Fickian and non-Fickian release from non-swelling devices in the form of slabs, spheres, cylinders or discs. *J. Control Release* **1987**, *5*, 23–36. [[CrossRef](#)]
17. Peppas, N.A. Analysis of Fickian and non-Fickian drug release from polymers. *Pharm. Acta Helv.* **1985**, *60*, 110–111.
18. Miller, K.V.; Noguera, R.; Beaver, J.; Medina-Plaza, C.; Oberholster, A.; Block, D.E. A Mechanistic Model for the Extraction of Phenolics from Grapes During Red Wine Fermentation. *Molecules* **2019**, *24*, 1275. [[CrossRef](#)] [[PubMed](#)]
19. Bychkov, A.L.; Podgorbunskikh, E.M.; Ryabchikova, E.I.; Lomovsky, O.I. The role of mechanical action in the process of the thermomechanical isolation of lignin. *Cellulose* **2018**, *25*, 1–5. [[CrossRef](#)]
20. Xing, Q.; Buono, P.; Ruch, D.; Dubois, P.; Wu, L.; Wang, W.-J. Biodegradable UV-Blocking Films through Core-Shell Lignin-Melanin Nanoparticles in Poly butylene adipate-co-terephthalate. *ACS Sustain. Chem. Eng.* **2019**, *7*, 4147–4157. [[CrossRef](#)]